



HAL
open science

Membrane contactors for intensified gas-liquid absorption processes with physical solvents: A critical parametric study

Laëtitia Cesari, Christophe Castel, Eric Favre

► To cite this version:

Laëtitia Cesari, Christophe Castel, Eric Favre. Membrane contactors for intensified gas-liquid absorption processes with physical solvents: A critical parametric study. *Journal of Membrane Science*, 2021, 635, pp.119377. 10.1016/j.memsci.2021.119377 . hal-03466835

HAL Id: hal-03466835

<https://hal.science/hal-03466835>

Submitted on 4 Apr 2023

HAL is a multi-disciplinary open access archive for the deposit and dissemination of scientific research documents, whether they are published or not. The documents may come from teaching and research institutions in France or abroad, or from public or private research centers.

L'archive ouverte pluridisciplinaire **HAL**, est destinée au dépôt et à la diffusion de documents scientifiques de niveau recherche, publiés ou non, émanant des établissements d'enseignement et de recherche français ou étrangers, des laboratoires publics ou privés.

***Membrane contactors for intensified gas-liquid absorption processes
with physical solvents: a critical parametric study***

Laëtitia Cesari, Christophe Castel, Eric Favre

Laetitia.cesari@univ-lorraine.fr

Laboratoire Réactions et Génie des Procédés, UMR 7274, Université de Lorraine, Nancy, France

Highlights:

- High intensification factors can be potentially achieved
- Key role of CO₂ solubility and solvent viscosity
- Different optimal module packing fraction are obtained
- Energy requirement has to be taken into account
- Intensification factors are independent of pressure

Abstract

Membrane contactors offer promising performances for the intensification of gas liquid absorption processes. Impressive volume reduction factors compared to packed columns have been reported, mostly for absorption in chemical solvents (e.g. CO₂ post combustion capture with MEA). A very limited number of studies addressed however the potentialities of membrane contactors for physical absorption processes. Moreover, the interplay between volume reduction and energy requirement, which is expected to be of major importance for physical solvents, is unexplored. In this study, a systematic parametric analysis of the intensification and specific energy requirement of membrane contactors for CO₂ absorption in 5 different physical solvents is reported. The best flow configuration, module packing fraction and membrane properties (mass transfer performances) are identified for the different solvents. Very high intensification factors compared to the baseline technology (i.e. packed column) are shown to be potentially achievable.

Keywords:

Membrane contactors, gas-liquid absorption, gas separation, physical solvents, intensification

List of parameters

Uppercase parameters

C	Concentration
C_p	heat capacities at constant pressure
C_v	heat capacities at constant volume
D	Diffusivity coefficient
D_{int}	Internal diameter of the membrane contactor
E	Energy
F	packing factor of the column
G_z	Graetz number
H_e	Henry coefficient
M	Molar mass
N_{fibers}	Number of fibers
N_{CO_2}	Molar flux of CO ₂
ΔP	Pressure drop
P	Pressure
Q	Molar flow
R	Ideal gas constant
Re	Reynolds number
Sc	Schmidt number
T	Temperature
V_i	Molar volume of the species i
Z	Length

Lowercase paremeters

a	Interfacial area
d_h	Hydraulic diameter
e	Membrane thickness
f	Pipe friction coefficient
k	Transfer coefficient
r	Radius of the fibers
u	Velocity

x Molar composition
y Molar composition

Greek parameters

α Selectivity
 ε Roughness factor
 μ Viscosity
 ρ Density
 φ Compacity of the membrane contactor
 σ Surface tension
 χ Association parameter in Wilke et Chang equation
 Ω Cross sectional area of the membrane contactor

1. Introduction

Membrane contactors are considered as one of the most promising technology for the intensification of gas-liquid absorption processes [1]. The use of modules equipped with highly gas permeable membranes and placed between the gas and liquid phase indeed offers unique possibilities compared to packed columns. The much larger specific surface area of membrane modules (5000 to 10 000 m²) compared to column packings (200-500 m²) opens the possibility to significantly decrease the size of the installation. The so-called intensification factor (I) which results from the volume reduction is one of the key interest of the technology [2–5]. A significant economy in terms of weight, because of the low density of polymers, can also be obtained; this characteristic can be of interest for off shore applications or mobile systems. Additionally, because no direct contact takes place between phases in a membrane contactor, the gas and liquid flowrates can be independently chosen. Consequently, a much larger ratio of gas / liquid velocities is possible and weeping or flooding phenomena are prevented. Nevertheless, several problems can limit the interest of membrane contactors; a low gas permeability material (such as a wetted hydrophobic membrane) and / or a low specific surface area module (i.e. large membrane diameter or low packing fraction) can lead a specific size of the unit which is larger than the baseline packing column case (i.e. $I < 1$). Moreover, pressure drop effects in hollow fiber modules are likely to significantly increase the energy requirement of the gas absorption process; a trade-off between process intensification and energy requirement has thus to be taken into account, but few studies addressed this point [6,7]. Membrane stability issues are also of importance, especially for harsh environments, such as chemical solvents.

Up to now, much effort has been made to investigate the potential of membrane contactors for gas-liquid processes based on chemical solvents, especially for carbon capture applications. The possibility to decrease the size of CO₂ postcombustion capture units is effectively of major interest. Numerous studies have been reported in order to evaluate the possibilities and limitations of membrane contactors for CO₂ capture with solvents such as MEA and MDEA, among others. The key role of membrane mass transfer performance, the strong impact of wetting effects and the materials stability issues have been highlighted. Through a series of modelling and simulation investigations, post-combustion membrane contactors can now be rigorously designed, with several pilot units tested with real flue gases.

Surprisingly, the same situation does not hold for gas liquid absorption processes based on physical solvents [8]. A large number of industrial units already make use however of physical solvents for a variety of gas purification applications, such as CO₂ removal from a pressurized gas mixture (hydrogen purification, precombustion carbon capture[9]). Absorption in a physical solvent is classically considered as the baseline technology for high pressure gas separation applications, with a pressure swing regeneration process to enable solvent recycling. Physical solvent processes are most often operated at high pressure in order to enhance the solubility of gases in the solvent and therefore generate a higher driving force. Even if the gas solubility decreases with a rise of temperature, physical solvents are also often operated at high temperature in order to reduce viscosity and pressure drop effects. The operating conditions, among other parameters, have a strong influence on the efficiency of the separation and can lead to an economical strategy, with optimal specifications for a given mixture [10]. Unfortunately, few studies have been reported on membrane contactors operated with physical solvents. In a pioneering study, Dindore et al [11] experimentally investigated the use of propylene carbonate in a hollow fiber membrane contactor for the removal of CO₂ at elevated pressure [12]. Their experiments showed that in the case of physical absorption the overall mass transfer is controlled by the liquid-side mass transfer resistance and morphological changes were observed inside the membrane, leading to a wetting of the fiber. More recently, some publications have explored pressurised water absorption (PWA) processes for biogas upgrading; the efficiency of 1D simulations to predict experimental separation performances and the predominant mass transfer resistance of the liquid phase have been shown. In order to circumvent the difficulties of porous materials observed by Dindore (membrane wetting is likely to occur due to the low surface tension of physical solvents and high pressure

conditions), dense skin membrane materials have been proposed [12]. Alternatively, ionic liquids are actively investigated for physical absorption processes and some preliminary results with membrane contactors have been reported [13]. The quantitative evaluation of the potentialities of membrane contactors in terms of process intensification are however essentially unexplored for the above applications.

This study intends to fill that gap through a systematic parametric study. Four solvents, which are commonly used in the physical absorption of CO₂: methanol (Rectisol process), N-methyl-2-pyrrolidone NMP (Purisol process), propylene carbonate (Fluor process), and polyethylene glycol dimethyl ether PGDE (Selexol process) [11,14,15] have been first selected. Because it is a cheap and green solvent with a high surface tension, water has been added for comparison purposes, despite its low CO₂ solubility [11]. Interestingly, these five different solvents show different CO₂ solubility performances [16] but also different physico-chemical properties (e.g. viscosity, density, surface tension ...). The impact of solubility and viscosity on intensification and energy requirement performances will thus be achievable. It can be anticipated that solvent viscosity is of importance for membrane contactor application, because operating conditions with physical solvents require a large specific liquid flowrate (compared to chemical solvents), leading to high pressure drop effects in a compact system. The intensification / energy requirement trade-off should thus to be systematically taken into account when membrane contactors are aimed for applications with physical solvents.

More specifically, the following questions will be addressed:

- What is the maximal intensification factor of membrane contactors for physical absorption processes compared to packed columns ?
- What are the best flow configurations (i.e. liquid flowing inside or outside the fibers), module design (packing factor), membrane performances (mass transfer coefficient) ?
- What is the interplay between intensification and specific energy requirement ?
- How do solvent viscosity and gas solubility impact the intensification performances ?

It will be shown that process intensification is not necessarily achieved with membrane contactors when applied to physical absorption processes ; moreover, the impact of solvent properties drastically changes the level of performances. Nevertheless, impressive volume reduction factors are attainable if specific guidelines for membrane and module design are used.

2. Overall framework of the study

The aim of the study is to explore the intensification potential of membrane contactors for physical absorption processes. It is expected that the possibilities offered strongly differ from the numerous studies reported up to now for chemical absorption processes. Indeed, given the major differences between physical and chemical absorption processes, summarized in Table 1, the interest of membrane contactors might be reconsidered:

- In terms of membrane performances, a very high membrane mass transfer coefficient (k_m) is needed for chemical solvents, because of the high liquid mass transfer coefficient. Typically, a 10^{-4} m.s⁻¹ or more value is recommended in order to maintain intensification potential. For lower values (such as obtained with wetted membranes), the membrane resistance becomes dominant and the interest of membrane contactors is questionable. For physical solvents, the liquid mass transfer coefficient is much lower (10^{-5} m.s⁻¹ or less); lower membrane mass transfer performances are thus required. This opens solutions such as dense selfstanding membranes which can withstand high pressure conditions [17,18].

- Chemical solvents are mostly aqueous solutions showing low viscosities. This leads to limited pressure drop effects on the liquid phase in membrane contactors. Conversely, the larger viscosity and much higher liquid/gas flowrate of physical absorption processes raises the question of excessive pressure drop levels in the liquid phase.
- Intensification factors around 4 have been reported for CO₂ post-combustion capture by chemical solvents with membranes contactors operated with real flue gases [19–21]. The pressure drop impact remains limited and module designs can fit the intensification / energy requirement trade-off [7]. The corresponding problem is unexplored for physical solvents.

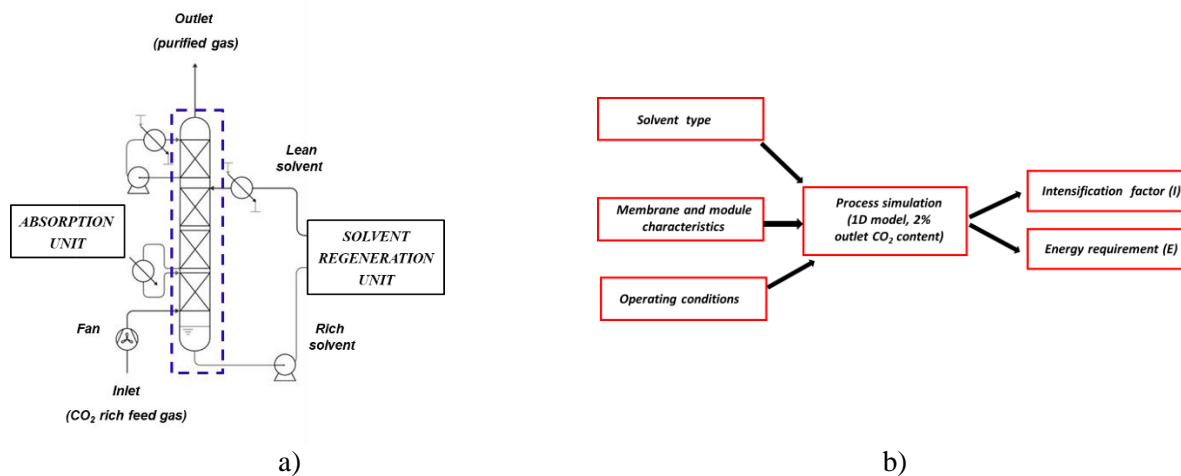
Table 1 : Major differences between physical and chemical absorption processes

		<i>Chemical</i>	<i>Physical</i>
<i>Mass transfer characteristics</i>	Liquid mass transfer coefficient (k_L)	High (enhancement due to chemical reaction)	Low
	Solvent viscosity	Low	High
<i>Operating conditions</i>	Specific liquid / gas flowrate	Low	High
<i>Membrane contactor performances</i>	Intensification factor (I)	Around 4	Unknown
	Energy requirement (kWh.Nm ⁻³)	Acceptable for adequate module design	Unknown

Figure 1 presents the synopsis of the study where :

- A membrane contactor unit is studied in order to replace a packed column used for CO₂ absorption by a physical solvent.
- The overall volume of the unit (dotted line) and the specific energy requirement will be compared depending on solvent type, membrane performances, module design and operating conditions.

Figure 1: Synopsis of the study.



The modelling and simulation strategy of the parametric study is detailed in the next section.

3. Modelling and parametric study

3.1 Properties of fluids

The properties of the five solvents at 25°C are listed in Table 2. The values of the CO₂ solubility in these solvents are taken from [11,16]. In this table, the Henry coefficient is defined as follows:

$$He_i = \frac{c_i^{gas}}{c_i^{liquid}} \quad (1)$$

Table 2: List of the investigated solvents and their properties at 25°C

Solvent	Usual name	Molar mass g.mol ⁻¹	Density kg.m ⁻³	Viscosity mPa.s	CO ₂ solubility -	CH ₄ solubility -
MeOH	Rectisol	32	785	0.6	0.32 ^a	6.17
DEPG	Selexol	280	1030	5.80	0.28 ^a	4.2
N-methyl-2-pyrrolidone (NMP)	Purisol	99	1027	1.65	0.28 ^a	3.9
Propylenecarbonate (PC)	Fluor solvent	102	1195	3.00	0.29 ^a	7.7
Water	Water	18	1000	1.00	1.22 ^b	28.8

a) from [16]

b) from [11]

The influence of temperature is investigated on propylene carbonate. The density and viscosity of the solvent have been taken from [22]. The Henry coefficient of CO₂ in propylene carbonate has been taken from Anouti et al for 333K [23] and from Murrieta-Guevara et al for 373K [24].

The determination of the diffusion coefficient and the diffusivity of gases in solvents were performed according to the methodology proposed by Dindore et al [12] which is described as follows.

The determination of the diffusivity of gases in the solvents at 25°C were calculated by the correlation of Diaz et al [25] as follows :

$$(D_{12})_{T=25^{\circ}C} = 6.02 \cdot 10^{-5} \cdot \frac{V_2^{0.36}}{\mu_2^{0.61} \cdot V_1^{0.64}} \quad (2)$$

With D_{12} the diffusivity coefficient of solute 1 in solvent 2 in $\text{cm}^2 \cdot \text{s}^{-1}$, V_2 and V_1 the molar volumes at normal boiling point temperature for gas (solute) and liquid (solvent) respectively in $\text{cm}^3 \cdot \text{mol}^{-1}$, μ the viscosity of the solvent in cP.

For other temperature, the diffusivity of gases in solvents has been calculated by the correlation of Wilke et Chang [26] :

$$(D_{12}) = 7.4 \cdot 10^{-8} \cdot \frac{\sqrt{\chi \cdot M \cdot T}}{\mu V^{0.6}} \quad (3)$$

Where D_{12} is the diffusivity coefficient of solute 1 in solvent 2 in $\text{cm}^2 \cdot \text{s}^{-1}$, M the molecular weight of the solvent, T the temperature in K, V the molar volume of the solute at normal boiling point temperature in $\text{cm}^3 \cdot \text{mol}^{-1}$, μ the viscosity of the solvent in cP. χ is the association parameter. For ordinary nonassociated solvents, $\chi = 1.0$. [26,27]

The molar volumes V_2 of the solvents at their normal boiling point were predicted by a groups contribution method described by Schotte. [28]

The diffusion coefficient of the binary mixture $\{\text{CO}_2 - \text{CH}_4\}$ was calculated by the Fuller equation [29]:

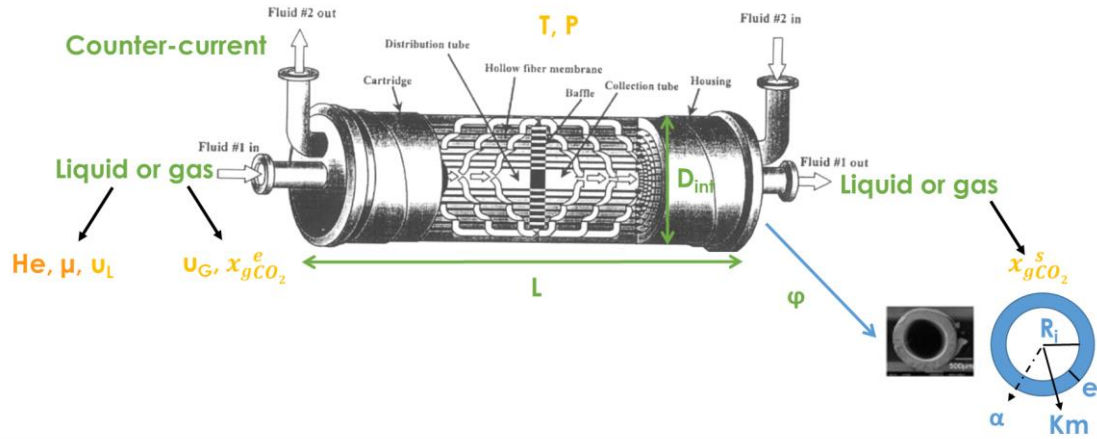
$$D_{AB} = \frac{0.00143 T^{1.75}}{P M_{AB}^{1/2} [(\sum v)_A^{1/3} + (\sum v)_B^{1/3}]^2} \quad (4)$$

Where D_{AB} is the binary diffusion coefficient in $\text{cm}^2 \cdot \text{s}^{-1}$, P is the pressure in bar, T the temperature in Kelvin, $\sum v$ is the summation of atomic diffusion volumes, M_A and M_B are the molecular weights of A and B, and $M_{AB} = 2 \left[\left(\frac{1}{M_A} \right) + \left(\frac{1}{M_B} \right) \right]^{-1}$.

3.2 Properties of membrane contactor

Numerous parameters can have an influence on the modelling of CO_2 physical absorption and must be taken into account in the parametric study. Figure 2 depicts a membrane contactor and the different parameters divided into four categories: parameters related to the membrane, to the contactor, to the solvent and the operating conditions.

Figure 2: Membrane contactor and its parameters adapted from [2].



The membrane fiber is characterised through its internal radius r_i , thickness e and mass transfer coefficient k_m (in $\text{m}\cdot\text{s}^{-1}$). Numerous studies addressed the impact of membrane mass transfer coefficient on membrane contactor performances. Typical values range between 10^{-4} to 10^{-5} for non wetted porous membranes or dense skin composite membranes. Thin dense selfstanding membranes can show k_m values close to 10^{-5} $\text{m}\cdot\text{s}^{-1}$ [30]. For wetted porous membranes, the mass transfer coefficient strongly decreases, down to 10^{-6} $\text{m}\cdot\text{s}^{-1}$.

The contactor can be operated in several configurations: co-current or counter-current and liquid-in or liquid-out. It is well known that the counter-current flow configuration is more efficient than the co-current one. Therefore, only the counter-current will be investigated in this work. However, choosing between the liquid-in or liquid-out configurations to obtain the best performances is always an issue. For this reason, both conformations are investigated in this work. The internal diameter of the contactor is fixed at 0.17 m, corresponding to a significant number of fibers and the length of the contactor is left variable and will be determined through the simulations. Finally, the module packing factor ϕ , corresponding to the volume fraction occupied by the fiber bundle over the overall membrane contactor volume, is investigated on a very large range, between 0.1 and 0.9.

The parameters related to the choice of the solvent are the solubility of CO_2 and the properties of the solvent (viscosity, density). As presented before, these parameters are listed in Table 2.

Finally, the operating temperature and pressure are fixed to 298.15K and 1 Bar respectively. The inlet gas enters the contactor with a 40/60 molar ratio of CO_2/CH_4 mixture at a volumetric flow of $1.39\cdot 10^{-2}$ $\text{Nm}^3\cdot\text{s}^{-1}$. The interstitial velocity ratio, defined as the liquid velocity over the gas velocity inside and outside the fibers, is investigated between 0.1 and 30. The outlet condition is a CO_2 molar fraction below 0.02 in the gas phase, typical of CO_2 purification targets (e.g. natural gas, biogas...) [31–33].

All the fixed and variable parameters investigated in this study and their values are listed respectively in Tables 3 and 4.

Table 3: List of fixed parameters and their value

Symbol	Parameter	Value	Unit
$Q_{\text{gas},0}$	Volume flow of gas at the entrance	0.0139	$\text{Nm}^3\cdot\text{s}^{-1}$
T	Temperature	298	K
R	Ideal gas constant	8.314	$\text{J}\cdot\text{mol}^{-1}\cdot\text{K}^{-1}$
α	Selectivity	1	/
D_{int}	Internal diameter of the module	0,17	m

$\varepsilon/(2r_{int})$	Roughness of the fiber	10^{-4}	
r_{int}	Hollow fiber internal radius	450	μm
e	Membrane thickness	50	μm
μ_g	Gas viscosity	10^{-5}	$\text{Pa}\cdot\text{s}^{-1}$
$D_{CO_2}^g$	Diffusion coefficient in gas phase	$1.78 \cdot 10^{-5}$	$\text{m}^2 \cdot \text{s}^{-1}$
$xg_{CO_2}^e/xg_{CH_4}^e$	Inlet CO_2/CH_4 molar ratio	0,4 / 0,6	/
$xg_{CO_2}^s$	Outlet CO_2 molar ratio	< 0,02	/

Table 4: List of variable parameters and their corresponding variation range

Symbol	Parameter	Value	Unit
φ	Module packing fraction	0.1 – 0.9	/
u_l/u_g	Interstitial velocity ratio	0.1 – 20	/
k_m	Membrane effective mass transfer coefficient	$10^{-3} - 10^{-5}$	$\text{m}\cdot\text{s}^{-1}$
P	Pressure	1 – 10	bar
/	Solvents	/	/
/	Configurations	/	/

3.3 Mass transfer

It is assumed that the membrane contactor is operated at steady state under isothermal conditions and no evaporation of the solvent. Moreover, the membrane mass transfer k_m is presumed constant. Finally, for both gas and liquid phases, plug flow conditions are settled. This set of condition is classically proposed for simulation purposes [34].

The interfacial area inside a_{in} and outside a_{out} the fiber and medium a_m , the hydraulic diameter of the fiber d_h , the log mean radius r_{ml} and the number of fibers are calculated according to:

$$a_{in} = \frac{2 \varphi r_{in}}{r_{out}^2} \quad a_{out} = \frac{2 \varphi}{r_{out}} \quad (5)$$

$$r_{ml} = \frac{e}{\log(r_{out}/r_{in})} \quad (6)$$

$$a_m = \frac{2 \varphi r_{ml}}{r_{out}^2} \quad (7)$$

$$d_h = \frac{2 r_{out} (1-\varphi)}{\varphi} \quad (8)$$

$$N_{fibers} = \frac{\Omega \varphi}{\pi r_{out}^2} \quad (9)$$

Where Ω is the section of the membrane contactor, r_{in} and r_{out} are the internal and external radius of the fibers.

The velocities and the dimensionless quantities Reynolds number Re , Schmidt number Sc and Graetz number Gz are defined for inside and outside the fibers as follows :

$$u_{in} = \frac{Q_{in}}{N_{fibers} \pi r_{in}^2} \quad u_{out} = \frac{Q_{out}}{\Omega (1-\varphi)} \quad (10)$$

$$Re_{in} = \frac{\rho_{in} u_{in} 2 r_{in}}{\mu_{in}} \quad Re_{out} = \frac{\rho_{out} u_{out} d_h}{\mu_{out}} \quad (11)$$

$$Sc_{in} = \frac{\mu_{in}}{\rho_{in} D_{in}} \quad Sc_{out} = \frac{\mu_{out}}{\rho_{out} D_{out}} \quad (12)$$

$$Gz_{in} = \frac{D_{in} Z}{u_{in} (2 r_{in})^2} \quad Gz_{out} = \frac{D_{out} Z}{u_{out} d_h^2} \quad (13)$$

Where Q , ρ , μ , D , u are the molar flow, density, viscosity, diffusion coefficient and velocity of the fluids. r_{in} is the internal radius of the fiber, d_h is the hydraulic diameter and Z the length of the contactor. The subscripts in and out refer to the inside or the outside of the fiber.

The determination of the transfer coefficient in the lumen and shell sides were determined using the same equations as used in our previous work [3,35] and are reminded below.

The determination of the Sherwood number inside the fibers was performed using the Graetz equations:

$$Sh_{in} = \begin{cases} 1.3 Gz_{in}^{(-1/3)} & \text{if } Gz_{in} < 0.03 \\ 4.36 & \text{if } Gz_{in} \geq 0.03 \end{cases} \quad (14)$$

On the shell side, the Sherwood number is determined for laminar flow ($Re < 500$) as before, using the Graetz [36] equations and for turbulent flow ($Re > 500$) by the correlation of Kartohardjono and Chen [37].

$$Sh_{out} = \begin{cases} 1.3 Gz_{out}^{(-1/3)} & \text{if } Re_{out} < 500 \text{ and } Gz_{out} < 0.03 \\ 4.36 & \text{if } Re_{out} < 500 \text{ and } Gz_{out} \geq 0.03 \\ (0.167 - 0.798\varphi + 1.738\varphi^2 - 1.370\varphi^3) Re_{out}^{0.7} Sc_{out}^{0.33} & \text{if } Re_{out} \geq 500 \end{cases} \quad (15)$$

The transfer coefficient inside k_{in} and outside k_{out} the fibers are defined according to:

$$k_{in} = \frac{Sh_{in} D_{in}}{2 r_{in}} \quad k_{out} = \frac{Sh_{out} D_{out}}{d_h} \quad (16)$$

The overall mass transfer coefficient is calculated according to a resistance in series approach [2] as follows:

$$\text{For liquid out:} \quad \frac{1}{K} = \frac{a_m}{k_{in} a_{in}} + \frac{1}{km} + \frac{He a_m}{k_{out} a_{out}} \quad (17)$$

$$\text{For liquid in:} \quad \frac{1}{K} = \frac{a_m}{k_{out} a_{ou}} + \frac{1}{km} + \frac{He a_m}{k_{in} a_{in}} \quad (18)$$

Finally, the evolution of the molar composition of CO_2 in the gas phase can then be determined by the resolution of the following differential equations:

$$\frac{d(Q_G y_i)}{dz} = K_G (C_i^{gas} - He_i \cdot C_i^{liquid}) a_m \Omega \quad (19)$$

$$Q_L \frac{dc_i^l}{dz} = K_G (C_i^{gas} - He_i \cdot C_i^{liquid}) a_m \Omega \quad (20)$$

with the following boundary conditions:

$$\begin{cases} y_i = y_{i,0} & z = 0 \\ C_i^l = C_i^{l,L} & z = L \end{cases} \quad (21)$$

Where Q_G and Q_L are the volume flows of gas and liquid respectively, y_i the molar composition of compound i and z the length of the contactor.

The average absorbed CO_2 molar flow can be calculated as follows:

$$N_{CO_2} = Q_{G,0} \cdot y_{CO_2,0} - Q_{G,L} \cdot y_{CO_2,L} \quad (22)$$

Where the subscripts 0 and L correspond to the entrance and the exit of the membrane contactor respectively.

3.4 Pressure drop

The pressure drop inside the fibers is given by the Hagen-Poiseuille expression

$$\Delta P_{in} = f \frac{\rho_{in} u_{in}^2 L}{4r_{in}} \quad (23)$$

Where f is the pipe friction coefficient.

According to the type of flow regime, the pipe friction coefficient f can be defined differently.

If the Reynolds number inside the fiber Re_{in} is lower than 2100 (corresponding to a laminar flow), then :

$$f = \frac{64}{Re_{in}} \quad (24)$$

Therefore, the pressure drop can be expressed as

$$\Delta P_{in} = 8u_{in}\mu_{in} \frac{L}{(r_{out}-e)^2} \quad (25)$$

For a turbulent flow (Re_{in} higher than 2100), the pipe friction coefficient f is defined as:

$$\frac{1}{\sqrt{f}} = -2 \log_{10} \left[\frac{2.51}{Re_{in} \sqrt{f}} + \frac{\varepsilon}{3.7(2r_{in})} \right] \quad (26)$$

Where ε is the roughness factor of fiber.

The latter can be evaluated by setting the value of the ratio $\varepsilon/(2r_{int})$, ranging from 10^{-6} (smooth pipe) to 0.05 (rough pipe).

Outside the fibers, the pressure drop is determined as follows:

$$\Delta P_{out} = 4K_o u_{out} \mu_{out} \varphi^2 \frac{L}{r_{out}^2(1-\varphi)} \quad (27)$$

where K_o (-) is the Kozeny constant, that can be evaluated as follows:

$$K = 150\varphi^4 - 314.44\varphi^3 + 241.67\varphi^2 - 83.039\varphi + 15.97 \quad (28)$$

3.5 Energy efficiency

The efficiency of each solvent and configuration is determined by the transferred CO₂ molar flow in comparison with its energy consumption. The transferred CO₂ molar flow is defined as the difference of the inlet and outlet CO₂ molar flows. The energy consumption is defined as the sum of the pressure drop in each phase, corresponding to the energy consumption of the compressor and the pump. The analytical expressions are given for each configuration.

$$\text{For liquid-out configuration: } P_{compr} = Q_g \frac{\gamma}{\gamma-1} \left(\frac{P+\Delta P_{in}}{P_0} \right)^{\left(\frac{\gamma-1}{\gamma} \right)} \quad (29)$$

$$P_{pump} = Q_l \Delta P_{out} \quad (30)$$

$$\text{For liquid in configuration: } P_{compr} = Q_g \frac{\gamma}{\gamma-1} \left(\frac{P+\Delta P_{out}}{P_0} \right)^{\left(\frac{\gamma-1}{\gamma} \right)} \quad (31)$$

$$P_{pump} = Q_l \Delta P_{in} \quad (32)$$

$$\text{With } \gamma = \frac{c_p}{c_v} \quad (33)$$

Where Q is the volumetric flow. The subscripts g and l correspond to the gas and liquid phases respectively. Cp and Cv are the heat capacities of the gas mixture at constant pressure and volume.

Packed column

For the packed column, taken as a baseline process here (Figure 1.a), simulations were performed at room temperature with the same inlet gas composition and flow. The influence of the pressure is investigated between 1 and 10 Bar and the operating point is set at 80% of the flooding area. The diameter of the packing dp_{pack} is set at 0.035 m with a specific area a of 140 m².m⁻³. Some relevant steps of the strategy are described below.

The column was design with the flooding determination by Eckert [38]:

$$Y_{flooding} = e^{(0.1117-4.012X^{0.25})} \quad (34)$$

$$X = \frac{u_L}{u_G} \sqrt{\frac{\rho_L}{\rho_G}} \quad (35)$$

$$u_{flooding} = \frac{1}{\rho_G} \sqrt{\frac{Y_{flooding} \rho_L \rho_G g}{F}} \quad (36)$$

Where F is the packing factor of the column fixed at 187 m².m⁻³.

$$\Omega = \frac{Q_g}{u_{flooding}^{0.8}} \quad (37)$$

The effective interfacial area is calculated at loading point according to Billet and Schultes [39]:

$$a_{eff} = 1.5 (a \cdot d_h)^{0.5} \left(\frac{\rho_L u_L d_h}{\mu_L} \right)^{-0.2} \left(\frac{u_L^2 \rho_L d_h}{\sigma_L} \right)^{0.75} \left(\frac{u_L^2}{g d_h} \right)^{-0.45} \quad (38)$$

Where σ_L is the surface tension of the liquid phase.

The determination of the transfer coefficient is performed through the calculation of the dimensionless numbers and the resistance in series approach:

$$Re_G = \frac{\rho_G u_G d_{pack}}{\mu_G} \quad Re_L = \frac{\rho_L u_L d_{pack}}{\mu_L} \quad (39)$$

$$Sc_G = \frac{\mu_G}{\rho_G D_G} \quad Sc_L = \frac{\mu_L}{\rho_L D_L} \quad (40)$$

$$Sh_G = 5.23. (a. dp_{pack})^{1.7} Re_G^{0.7} Sc_G^{0.23} \quad (41)$$

$$k_G = \frac{Sh_G D_G}{d_{pack}} \quad (42)$$

$$k_L = 0.0051 \left(\frac{\mu_L g}{\rho_L}\right)^{0.33}. (a. dp_{pack})^{-0.27} Re_L^{0.65} Sc_L^{-0.5} \quad (43)$$

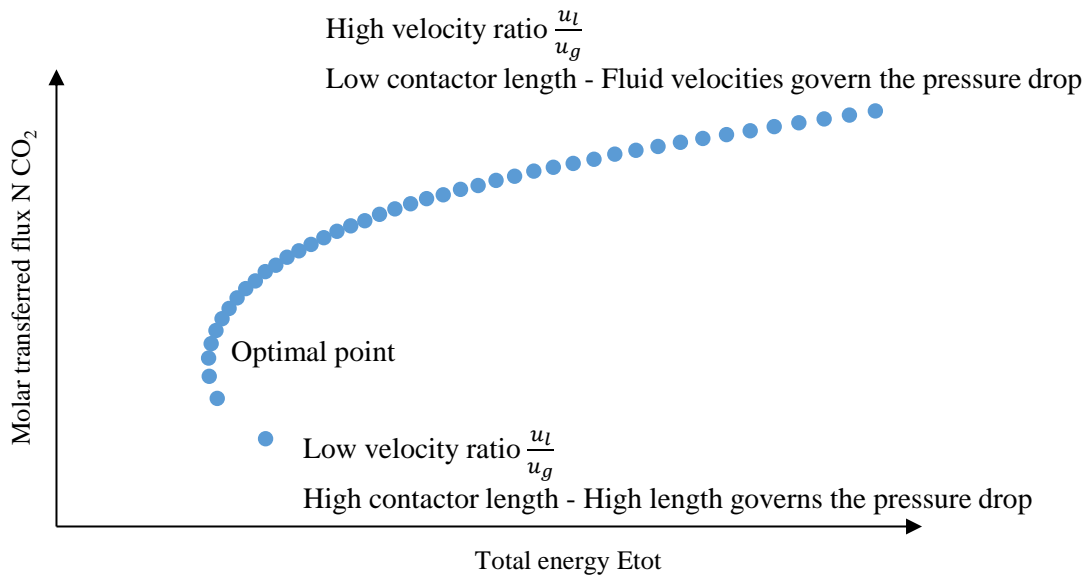
$$K_G = \frac{1}{\frac{1}{k_G} + \frac{H_e}{k_L}} \quad (44)$$

4. Results and discussion

4.1 Influence of parameters

The evaluation of the solvent's performance is determined by the value of the molar flow of CO₂ transferred as a function of the total energy consumption. In our case, the total energy consumption is mostly caused by the pressure drop in the liquid side. A completely different situation is obtained with chemical solvents, where pressure drop on the gas side are usually dominant. Each curve shows the same pattern with an optimal point in term of energy consumption (not always depicted in graphs). A schematic representation is depicted in Figure 3. Each point corresponds to a different velocity ratio. At very low velocity, the transfer is not efficient enough and a huge length of the fiber is required leading to an elevated pressure drop. When the velocity increases, the transfer is favoured, leading to a shorter fiber and a lower pressure drop. After the optimal point, the transfer is still favoured by the rise of the velocity, but this latter generates a rise in the pressure drop.

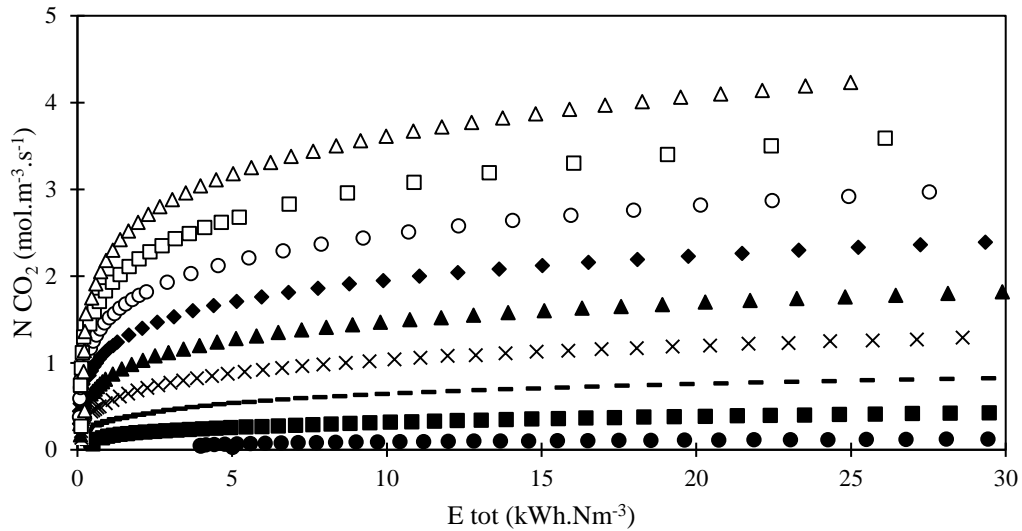
Figure 3: Decomposition of the different regimes



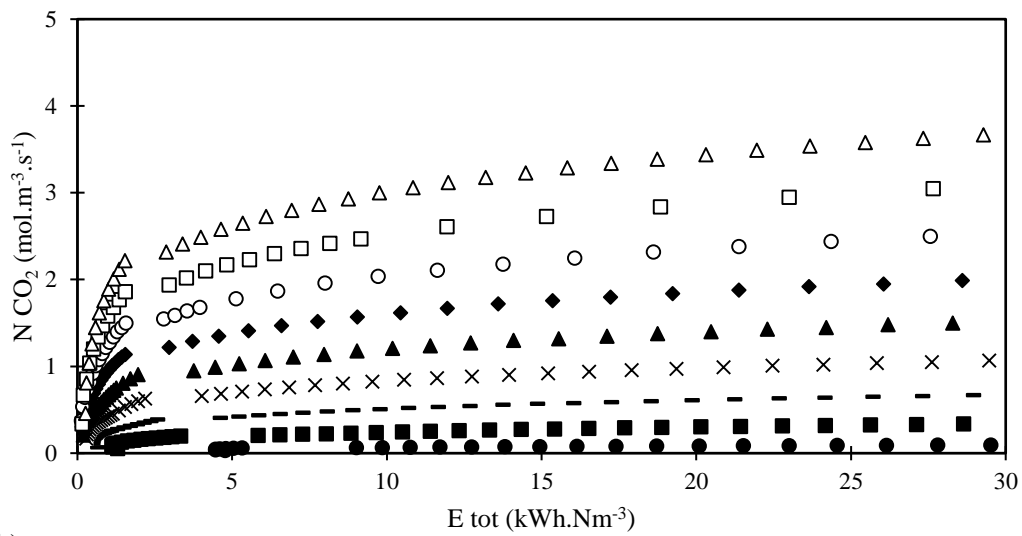
4.2 Influence of solvent properties

Figure 4 shows the results for the five studied solvents at different packing fraction values for a mass coefficient transfer k_m fixed at 10^{-3} m.s^{-1} and a liquid-in configuration. At first glance, it can be observed that Selexol and water show the lowest performances for the set of specifications fixed for CO_2 purification. Indeed, the molar flows of CO_2 transferred are the lowest with a very large energy requirement. When looking at low energy values, the performance of the solvents decreases as follows methanol > NMP > PC > Selexol > water. The same trend is observed for the k_m values of 10^{-4} and 10^{-5} m.s^{-1} and for the liquid out configuration also. These results can be explained by the low CO_2 solubility in water and by the high viscosity of Selexol. Indeed, an increase of the viscosity will lead to a diminution of the CO_2 flux and a high energy consumption. Looking at the viscosity of Rectisol, NMP, PC and Selexol, it can be noticed that the performances of these solvents follow the reverse tendency of the viscosity. Moreover, the CO_2 solubility appears to be a critical parameter. Indeed, PC and water seems to have similar physical properties. However, the solubility of CO_2 in water is 4 times lower than in PC. The CO_2 transferred flux is not in the same order of magnitude: the value is 10 times higher for PC than for water at the same energy consumption. Hence, a low CO_2 solubility will lead to higher impact on the energy efficiency than a high viscosity.

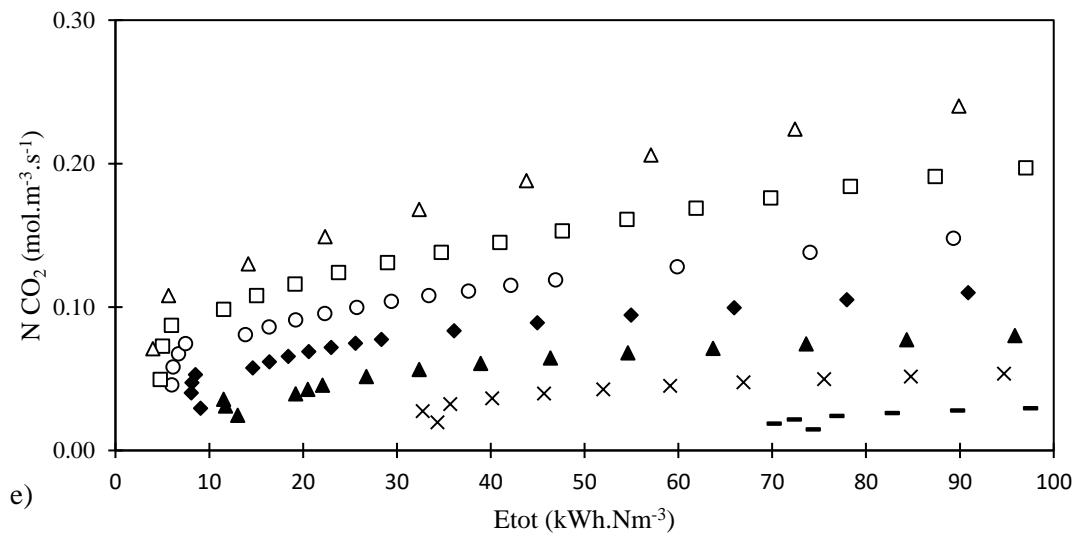
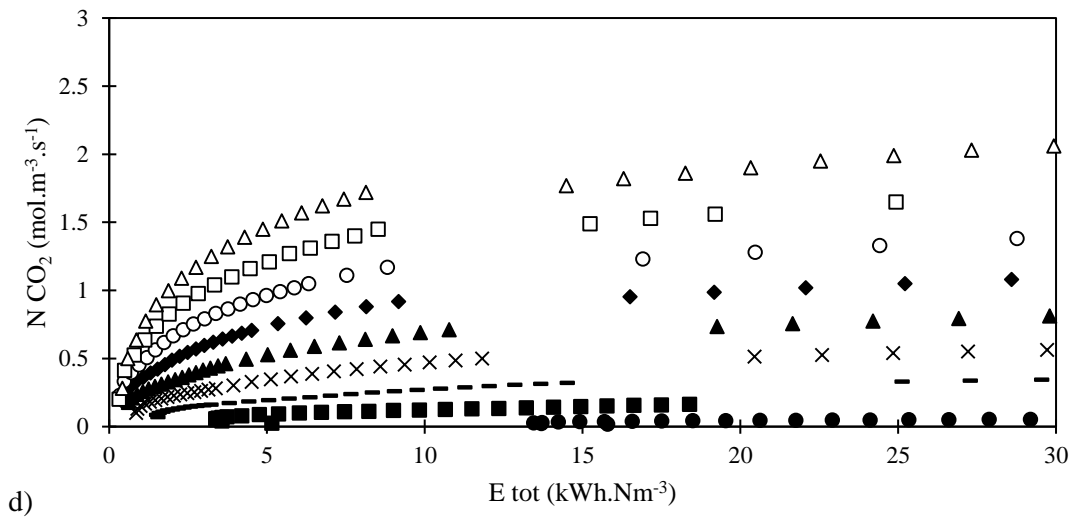
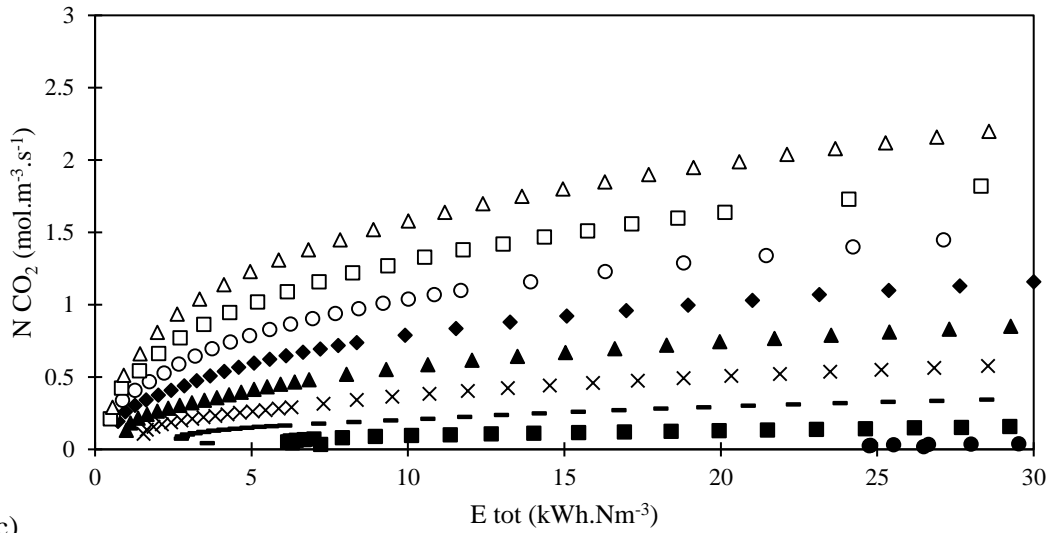
Figure 4: Generic overview of simulation results for 5 solvents with increasing packing factor: molar flow of CO₂ transferred as a function of the total energy with a k_m value of 10^{-3} m.s⁻¹ for the liquid in configuration. Figure a) methanol (Rectisol), b) NMP (Purisol), c) DEPG (Selexol), d), propylene carbonate (Fluor solvent), e) water. ϕ values : ● : 0.1 ; ■ : 0.2 ; — : 0.3 ; × : 0.4 ; ▲ : 0.5 ; ◆ : 0.6 ; ○ : 0.7 ; □ : 0.8 ; △ : 0.9.



a)



b)



4.3 Influence of membrane performances

In addition to the liquid side, performances can also be affected by the value of the membrane transfer coefficient k_m . The value of k_m was investigated between 10^{-3} and 10^{-5} m.s^{-1} for the five solvents. Results in Table 5 are given for the liquid in configuration with a module compacity (packing fraction) of 0.5 and u_l/u_g ratio of 2. As expected, a higher value of the k_m coefficient leads to a better CO_2 transferred flux and a lower energy consumption for all the solvents. One can observe that the most efficient solvents (methanol and NMP) are the most affected by the decrease of the k_m value. Moreover, it can be highlighted that a decrease of the k_m value from 10^{-3} to 10^{-4} m.s^{-1} leads to a smaller variation of the energy consumption and transferred flux than a decrease of the k_m value from 10^{-4} to 10^{-5} m.s^{-1} . For example, the ratio of transferred flux over energy consumption for methanol is divided by 4 (transferred flux divided by 2, energy consumption multiplied by 2) when the value of k_m drops from 10^{-3} to 10^{-4} m.s^{-1} . For a change from 10^{-4} to 10^{-5} m.s^{-1} , the ratio for methanol goes down to 25 (transferred flux divided by 5, energy consumption multiplied by 5). On the other hand, water is only slightly altered by the modification of k_m . Indeed, the transfer coefficient value in the liquid side is quite low meaning that the liquid side is more limiting than the membrane.

Table 5: Comparison of the influence of the k_m value: $10^{-3} - 10^{-5}$ m.s^{-1} . Results are given for a compacity of 0.5 and u_l/u_g ratio of 2.

k_m (m.s^{-1})		MeOH	NMP	PC	Selexol	Water
10^{-3}	k_l (m.s^{-1})	$1.83 \cdot 10^{-5}$	$1.43 \cdot 10^{-5}$	$9.06 \cdot 10^{-6}$	$8.96 \cdot 10^{-6}$	$8.24 \cdot 10^{-6}$
	E_{tot} (kWh.Nm^{-3})	0.896	1.25	3.69	6.83	22.0
	$N \text{ CO}_2$ ($\text{mol.m}^{-3}.\text{s}^{-1}$)	$8.11 \cdot 10^{-1}$	$7.50 \cdot 10^{-1}$	$4.61 \cdot 10^{-1}$	$4.82 \cdot 10^{-1}$	$4.55 \cdot 10^{-2}$
10^{-4}	k_l (m.s^{-1})	$1.7 \cdot 10^{-5}$	$1.17 \cdot 10^{-5}$	$7.83 \cdot 10^{-6}$	$7.74 \cdot 10^{-6}$	$8.24 \cdot 10^{-6}$
	E_{tot} (kWh.Nm^{-3})	1.68	2.27	5.71	10.6	23,6
	$N \text{ CO}_2$ ($\text{mol.m}^{-3}.\text{s}^{-1}$)	$4.32 \cdot 10^{-1}$	$4.15 \cdot 10^{-1}$	$2.98 \cdot 10^{-1}$	$3.11 \cdot 10^{-1}$	$4.25 \cdot 10^{-2}$
10^{-5}	k_l (m.s^{-1})	$1.7 \cdot 10^{-5}$	$1.21 \cdot 10^{-5}$	$7.80 \cdot 10^{-6}$	$7.51 \cdot 10^{-6}$	$8.24 \cdot 10^{-6}$
	E_{tot} (kWh.Nm^{-3})	8,12	10.3	20.8	39.2	38,2
	$N \text{ CO}_2$ ($\text{mol.m}^{-3}.\text{s}^{-1}$)	$8.99 \cdot 10^{-2}$	$9.2 \cdot 10^{-2}$	$8.18 \cdot 10^{-2}$	$8.44 \cdot 10^{-2}$	$2.62 \cdot 10^{-2}$

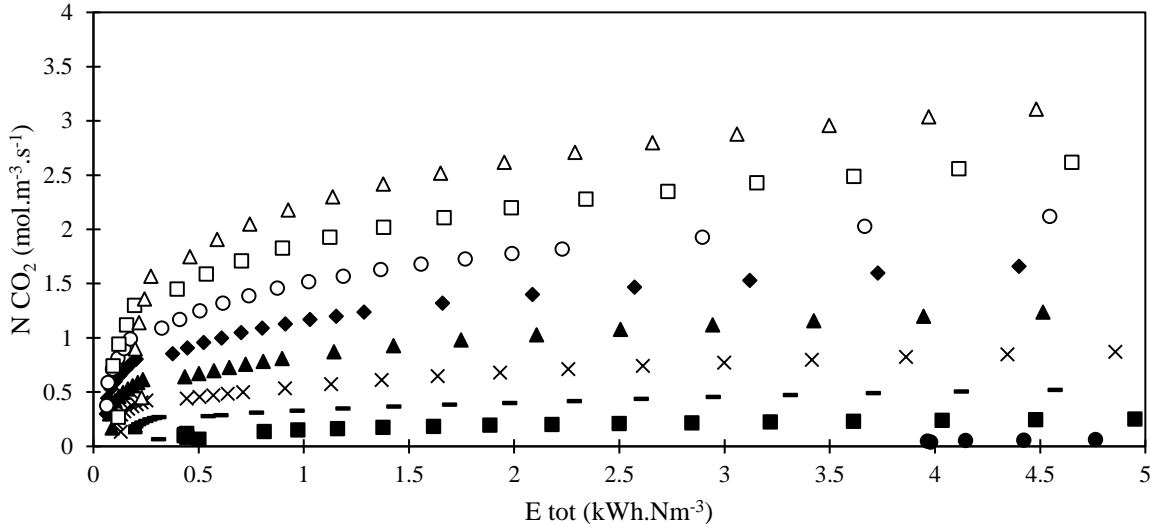
The investigation on the influence of the membrane transfer coefficient k_m logically shows that the higher the value, the better the absorption performances. A value of k_m around 10^{-3} and 10^{-4} m.s^{-1} seems ideal for physical solvents. A lower value (e.g. 10^{-5} m.s^{-1}) will lead to a limitation by the membrane. Therefore, for porous membranes, it remains essential to avoid any process such as membrane wetting that could decrease the k_m value. Alternatively, thin skin composite membranes, which are not impacted by wetting problems, can achieve k_m values around 10^{-4} m.s^{-1} , while dense selfstanding membranes seem limited to 10^{-5} m.s^{-1} .

4.4 Influence of flow configuration (liquid in or liquid out)

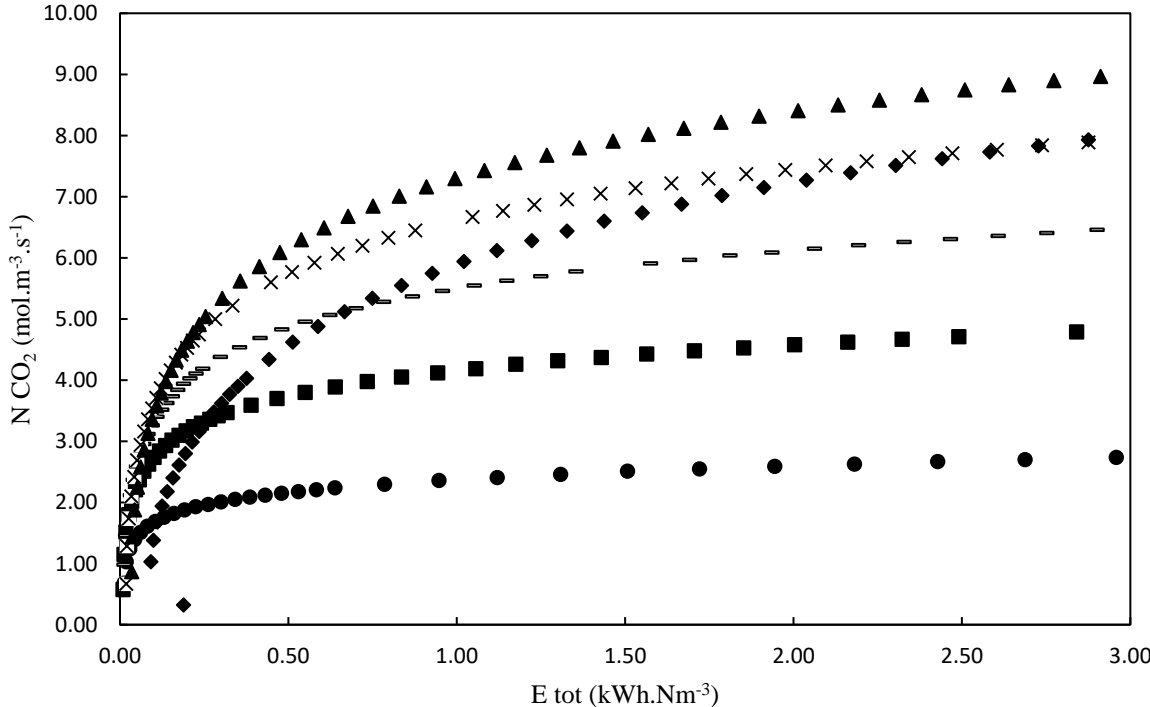
The influence of the configuration – liquid-in or liquid-out – on the overall efficiency for several packing fraction values is depicted with methanol as example in Figure 5. In the liquid-in configuration, the CO_2 transferred flow increases and the energy consumption decreases as the packing fraction increases. Since the number of fibers in the module increases, the specific area increases therefore improves the transfer. In the meantime, the velocity in each fiber decreases, diminishing the pressure drop in the liquid side. In the liquid-out configuration, a different phenomenon is found. An increase of the packing factor values from 0.1 to 0.5 will increase the transfer due to the increase of the specific area. However, with a value of 0.6 and higher, the efficiency of the transfer decreases drastically with a rise of the energy consumption caused by a higher pressure drop in the liquid side. Similar effects are observed for all

solvents but for different values of compacity (module packing fraction). Thus, the compacity shows an optimum value that is strongly depending of the solvent used. To our knowledge, no study reported up to now the occurrence of optimal module packing fractions for membrane contactors as a function of solvent properties. This result is important for future membrane contactor design strategies.

Figure 5: Molar flow of CO₂ transferred as a function of the total energy for methanol with a Km value of 10⁻³ m.s⁻¹ for a) liquid in configuration; b) liquid out configuration. φ values : ● : 0.1 ; ■ : 0.2; — : 0.3 ; × : 0.4; ▲ : 0.5 ; ◆ : 0.6 ; ○ : 0.7; □ : 0.8 ; Δ : 0.9.



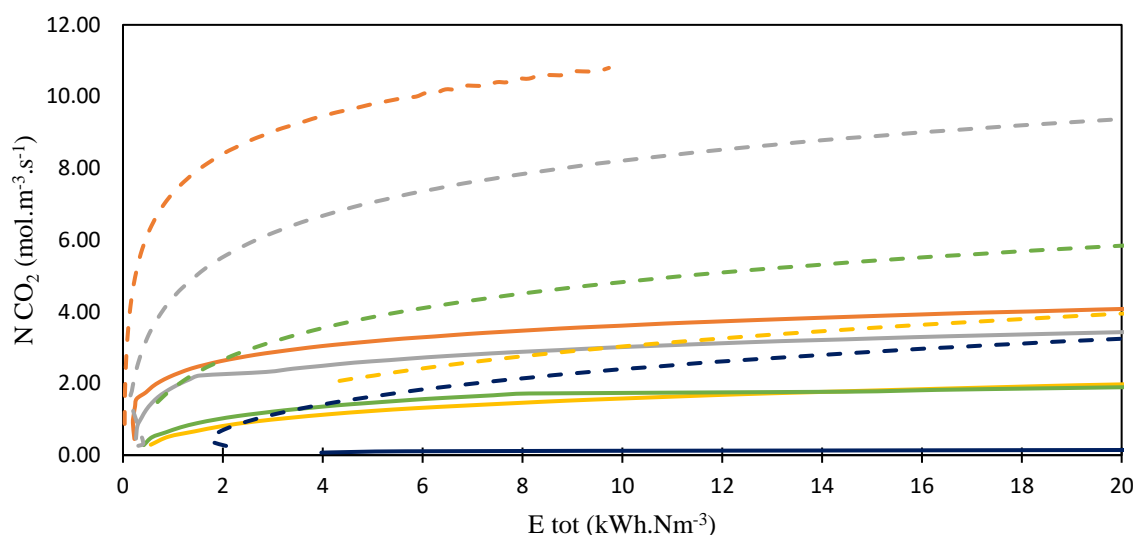
a)



b)

The choice of the liquid-in or liquid-out configuration has always been an issue for the use of membrane contactors. In Figure 6, the maximal CO₂ absorption fluxes are represented for each solvent and configuration, namely with a k_m value of 10^{-3} m.s⁻¹ and a compacity of 0.9 for liquid-in configuration and the optimum value for liquid-out configuration. It can be noticed that for all solvent, the liquid-out configuration is the most efficient. The difference is the most impressive for the most efficient solvent (methanol and NMP). The fact that liquid out configuration offers the best performances whatever solvent type is noticeable and should be taken into account for future studies. However, it is important to note that the prediction of pressure drop and mass transfer coefficients on the shell side of membrane contactors is complex. Numerous correlations have been already proposed, depending on fiber geometry and packing fraction, among others. Different correlations will necessarily quantitatively modify the pressure drop and mass transfer predictions. A detailed analysis of the impact of different correlations on performances would be of interest but it is outside the scope of this study. We think however that the systematic liquid out option suggested above remains robust whatever the membrane module simulation strategy.

Figure 6: Maximum CO₂ flow for each solvent with K_m value fixed at 10^{-3} m.s⁻¹. Blue: water; orange: methanol; grey: NMP; yellow: Selexol; green : PC., Continuous lines: liquid in configuration (compacity of 0.9); dotted lines: liquid out configuration (compacity of 0.5)



It should be also stressed that membrane mechanical properties will play a key role, given the pressure drop levels; more specifically, the fibers are subjected to a risk of crushing for the liquid-out configuration or bursting for the liquid-in configuration.

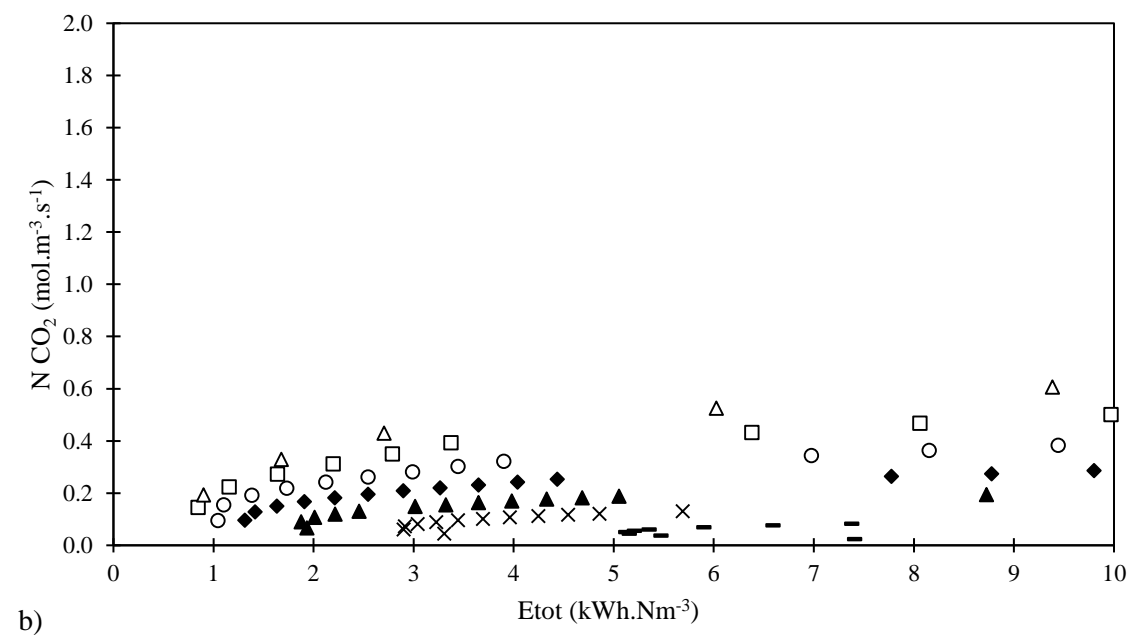
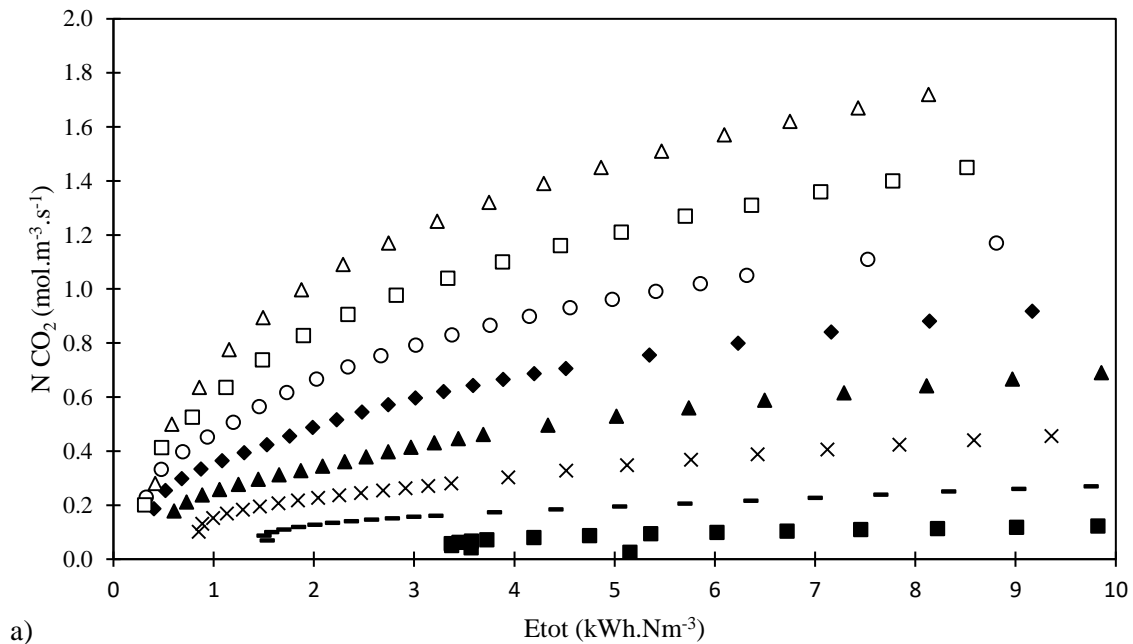
4.5 Influence of pressure and temperature

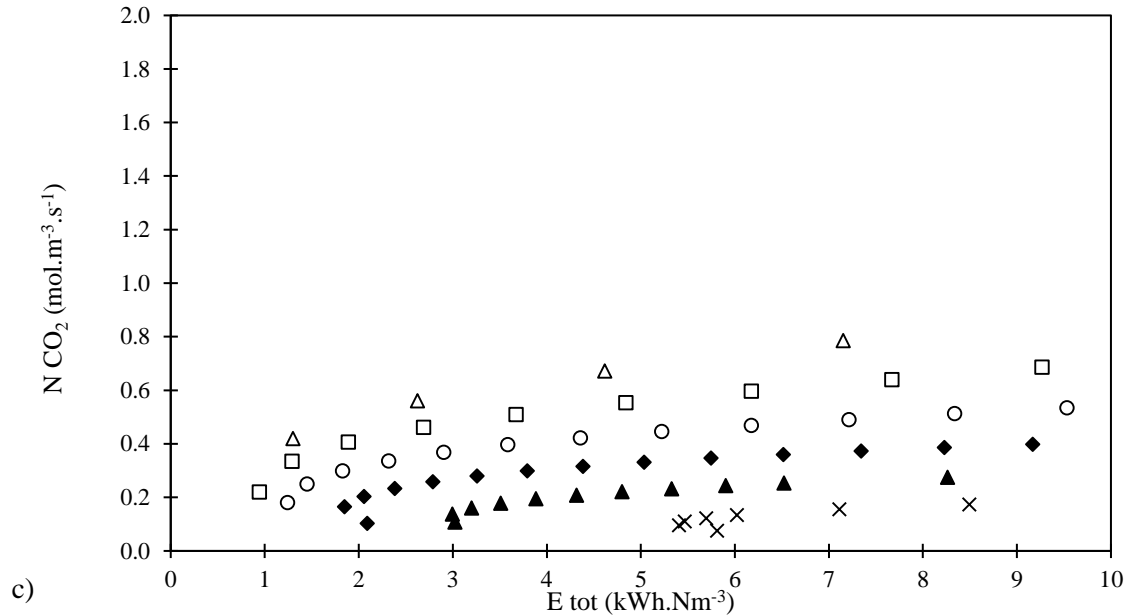
As presented in the introduction of the article, physical solvent processes generally operate at high pressure to favour the solubility of gases in solvent and improve the driving force. On the other hand, the diffusivity coefficient and solvent properties are not significantly impacted by pressure.

Temperature has a very strong impact on several parameters in physical solvent processes. From a mass transfer coefficient point of view, an increased temperature will be interesting because of the lower viscosity of the solvent. This has to be however balanced by the simultaneous decreased gas solubility,

that is a lower driving force. Because gas-liquid absorption flux depends on the product of driving force and mass transfer coefficient, it is interesting to study the influence of temperature. This is especially true for systems which show a major mass transfer resistance in the liquid, that is for high membrane mass transfer coefficients. Figure 7 shows the results for propylene carbonate for 3 different temperature levels: 298 K, 333K and 373 K.

Figure 7: Molar flow of CO₂ transferred as a function of the total energy for propylene carbonate in liquid in configuration with a Km value of 10⁻³ m.s⁻¹ for several temperature a) T = 298K, b) T = 333K, c) T = 373K. φ values : ● : 0.1 ; ■ : 0.2; — : 0.3 ; × : 0.4; ▲ : 0.5 ; ◆ : 0.6 ; ○ : 0.7; □ : 0.8 ; △ : 0.9.





It first can be noticed that membrane contactor with low capacity (ϕ values below 0.4) can only be operated at low temperature for a reasonable energy consumption (below 10 kWh.Nm⁻³). Moreover, high CO₂ absorption fluxes can be achieved for low temperature conditions (Figure 7a). With an increase of temperature up to 333K (Figure 7b), CO₂ absorption flux shows an important decrease, but at high temperature (Figure 7c), the values of CO₂ flows are surprisingly slightly higher. These results demonstrate that the solubility of gases in solvent is the governing parameter that must be the higher as possible to achieve maximal mass transfer. Thus, it is advised to operate with a low or ambient temperature. Secondly, the temperature must be high enough to have a significant impact on the solvent properties, especially the viscosity, and on the diffusivity coefficient. With only a small increase of temperature, physical solvent process presents a lose/lose situation with low gas solubility, low diffusivity coefficient and high viscosity. Anyways, the physical properties and diffusivity advantages at high temperature cannot compensate the loss due to the solubility. These results are obtained for propylene carbonate solvent but similar phenomena are expected to hold for other solvents. The combination of gain and loss with temperature requires a full study with strategic parameters for a given mixture.

4.6 Comparison with packed columns: Intensification possibilities

As previously presented, the membrane contactor presents numerous advantages in comparison with the packed column. One major objective of this study is to compare the two technologies in term of specific volume (i.e. specific CO₂ absorption fluxes). Results of the packed column, the baseline case are presented in Table 6. As for the membrane contactor, the same performance tendency is obtained for the five solvents: methanol > NMP > PC > selexol > water. The absorption fluxes logically increase with a rise of the pressure, together with an increased energy requirement.

Table 6: Results for packed column

Solvent	Pressure bar	Gas feed flow $\text{Nm}^3.\text{s}^{-1}$	Liquid flow $\text{m}^3.\text{h}^{-1}$	Column diameter m	ul/ug -	Column height m	CO_2 flow $\text{mol.m}^{-3}.\text{s}^{-1}$	Column volume m^3
Methanol	1	0.0139	20.47	0.36	0.37	3.91	0.56	0.41
	5	0.0139	4.09	0.18	0.37	3.40	2.76	0.08
	10	0.0139	2.05	0.13	0.37	3.20	5.26	0.04
NMP	1	0.0139	18.25	0.34	0.33	6.68	0.37	0.62
	5	0.0139	3.65	0.17	0.33	6.02	1.75	0.13
	10	0.0139	1.83	0.12	0.33	5.73	3.32	0.07
PC	1	0.0139	19.17	0.35	0.35	9.44	0.25	0.91
	5	0.0139	3.83	0.17	0.35	8.70	1.19	0.19
	10	0.0139	1.92	0.12	0.35	8.34	2.26	0.10
Selexol	1	0.0139	18.12	0.34	0.33	17.57	0.14	1.62
	5	0.0139	3.62	0.17	0.33	16.33	0.65	0.35
	10	0.0139	1.81	0.12	0.33	15.66	1.22	0.19
Water	1	0.0139	79.47	0.76	1.43	4.35	0.12	1.97
	5	0.0139	15.89	0.32	1.43	4.34	0.66	0.34
	10	0.0139	7.95	0.22	1.43	4.30	1.35	0.17

The intensification factor I can then be evaluated, through the volume ratio of the packed column over the membrane contactor. A series of data is reported in Table 7 for a 1 Bar inlet pressure and a maximal energy requirement of 1 kWh/Nm^3 . For all solvents, both liquid-in and liquid-out configurations are equivalent or better than the packed column. Interestingly, the maximal intensification factors are obtained for the maximal module packing fraction (0.9), while a variable optimal packing fraction is required for the liquid out configuration (0.2 to 0.5). Moreover, the highest I values are systematically obtained for the liquid out configuration, and the optimal module packing factor increases with a decrease of the solvent viscosity. The possibility to achieve impressive intensification factors is clear: for a 1 Bar inlet pressure, intensification factors reach values of 13.3 for methanol, 11.9 for NMP, 8.56 for PC, 8.07 for selexol and 7.08 water. Methanol thus offers the highest intensification possibilities, due to a shorter contactor length and a higher velocity ratio. However, methanol is also the only solvent to develop a turbulent regime for this value of energy consumption.

Table 7: Highest values of N_{CO_2} for a total energy consumption E_{tot} around a value of 1 kWh.Nm^{-3} (Temperature = 298K, Pressure = 1 bar).

Solvent	Configuration	ϕ value -	Z m	N_{CO_2} $\text{mol.m}^{-3}.\text{s}^{-1}$	u_l/u_g -	u_l m.s^{-1}	I
Methanol	Liquid in	0.9	4.62	2.30	0.5	3.39	4.11
	Liquid out	0.5	1.44	7.43	5.0	8.36	13.3
NMP	Liquid in	0.9	5.65	1.89	0.4	2.71	5.11
	Liquid out	0.5	2.42	4.41	2.25	3.76	11.9
PC	Liquid in	0.9	13.72	0.78	0.2	1.35	3.12
	Liquid out	0.4	4.98	2.14	1.3	2.72	8.56
Selexol	Liquid in	0.9	20.7	0.51	0.1	0.677	3.64
	Liquid out	0.3	9.46	1.13	0.7	1.95	8.07
Water	Liquid in	-	-	-	-	-	-
	Liquid out	0.2	12.5	0.85	1.4	5.85	7.08

The impact of pressure on the maximal intensification factor is also of interest and it has been explored through a parametric study. Simulations have been performed at 1, 5 and 10 Bar gas pressure for the liquid in configuration. Results are shown in Table 8 for the following conditions: $u_l/u_g = 1$, $\phi = 0.9$, $k_m = 10^{-3} \text{ m.s}^{-1}$. The driving force being proportional to the pressure, a rise of the pressure implies a rise of the CO_2 absorption flux. In the same way, the length of the contactor required to obtain the outlet 2% CO_2 composition is shortened. Consequently, the total energy consumption also decreases. Table 8 also presents the calculations of the intensification factor of the CO_2 molar transferred flow for the liquid in configuration of the membrane contactor in comparison with the packed column at the same gas pressures (1, 5 and 10 bars). For each solvent, the intensification factor remains globally the same for different pressures. These results imply that for a first approach, the intensification factor I are transposable in pressure.

Table 8: Influence of the pressure in liquid-in configuration ($u_l/u_g = 1$, $\phi = 0.9$, $k_m = 10^{-3} \text{ m.s}^{-1}$).

Solvent	Gas pressure bar	Z m	N CO_2 $\text{mol.m}^{-3}.\text{s}^{-1}$	Etot kWh.Nm^{-3}	I -
Methanol	1	3.35	3.18	5.03	5.68
	5	0.67	15.9	$6.69 \cdot 10^{-2}$	5.76
	10	0.34	31.8	$8.67 \cdot 10^{-2}$	6.05
NMP	1	3.64	2.93	8.75	7.92
	5	0.73	14.7	$8.6 \cdot 10^{-2}$	8.40
	10	0.36	29.3	$8.91 \cdot 10^{-2}$	8.83
PC	1	5.72	1.86	18.3	7.44
	5	1.14	9.31	0.142	7.82
	10	0.57	18.6	$9.61 \cdot 10^{-2}$	8.23
Selexol	1	5.47	1.95	19.1	13.93
	5	1.09	9.75	0.211	15.00
	10	0.55	19.5	0.105	15.98
Water	1	44.3	0.24	89.9	2.00
	5	8.86	1.20	0.298	1.82
	10	4.43	2.40	0.118	1.78

The impact of temperature has also been investigated on the intensification factor I . Simulations have been performed at 298, 333 and 373 K on membrane contactor and packed column are results are presented in Table 9. As previously shown in section 4.6, for the membrane contactor, a rise of temperature implies two opposite phenomena: better transfer and low viscosity of the solvent, but also a lower solubility of the gas. In the packed column, the low solubility of gas with the increasing temperature requires a high velocity ratio u_l/u_g that completely modify the design of the column. Therefore, the packed column is more efficient at high temperature with a lower height and a higher CO_2 transferred flow. Contrary to the pressure, the intensification factor is strongly temperature dependent and the higher I values are achieved at the lower temperature.

Table 9: Influence of the temperature – comparison with packed columns for propylene carbonate. Membrane contactor parameters: liquid in configuration, $u_l/u_g = 1$, $\phi = 0.9$, $k_m = 10^{-3} \text{ m.s}^{-1}$.

Temperature K	Membrane contactor			Packed column				I
	Z m	N_{CO_2} $\text{mol.m}^{-3}.\text{s}^{-1}$	E_{tot} kWh.Nm^{-3}	Diameter m	Height m	N_{CO_2} $\text{mol.m}^{-3}.\text{s}^{-1}$	u_l/u_g -	
298	5.72	1.86	18.3	0.350	9.44	0.251	0.35	7.44
333	11.8	0.90	40.5	0.496	4.14	0.285	0.62	3.16
373	8.75	1.22	30.2	0.691	1.35	0.452	1.00	2.70

5. Conclusion

This study intended to explore the possibilities of process intensification thanks to membrane contactors for absorption processes based on physical solvents. A systematic parametric study has been performed for CO_2 absorption in five different solvents showing a broad range of solubility and viscosity.

The main conclusions can be summarized as follows:

- Membrane contactors offer promising intensification possibilities compared to a classical packed column with volume reduction ratios up to 15
- The maximal intensification factor I is almost independent of the inlet pressure
- The liquid out configuration systematically shows the highest intensification factor, providing that an optimal module packing fraction is used. The optimal module fraction depends on solvent properties and range between 0.2 for low viscosity solvents and 0.5 for high viscosity solvents
- For the liquid in configuration, the optimal module packing fraction is always maximal (i.e. 0.9 in this study)
- The membrane mass transfer performances are of major importance, both for the intensification performances and specific energy requirement. The effective membrane mass transfer coefficient k_m should ideally be above 10^{-5} , or better, 10^{-4} m.s^{-1} in order to achieve maximal intensification performances. Interestingly, numerous studies have reported experimental data that fit this range, be it with porous, thin film composite or dense selfstanding membranes. Nevertheless, the interest of membrane contactors drastically decreases for values below 10^{-5} m.s^{-1} . This data is typical of porous, wetted membrane materials.
- Increasing the specific absorption fluxes (i.e. pushing the intensification factor) systematically increases the energy requirement, through a non linear relationship. The energy requirement is largely dominated by the liquid pressure drop effect, at the difference of membrane contactors for chemical absorption systems (for which a moderate gas side pressure drop is the dominant energy requirement term). Given the much larger energy requirement data obtained for physical solvents, the intensification / energy requirement trade-off is thus of major importance and should be systematically taken into account. A technico-economical analysis is necessary in order to identify the best balance between large intensification factors (i.e. lower CAPEX) and increased energy requirement (i.e. larger OPEX).
- Finally, the solvent properties also play a role on the overall process performances, both for the intensification possibilities and energy requirement impact. A high solubility and low viscosity

should logically be favoured; this statement explains why Rectisol (methanol) lead to the best performances among the five solvents investigated in this study.

Beyond the above conclusion, this study suggests several perspectives for future work.

The interest of membrane contactors for other applications or different solvents could be also investigated. The results obtained here show however that solvent viscosity strongly impacts the interest and feasibility of membrane contactors compared to packed columns. To that extend, it is likely that high viscosity solvents such as ionic liquid, glycerol or oils, used for gas drying, gas purification or VOC recovery applications poorly fit the requirements for membrane contactors to be of interest.

Because the solubility / viscosity interplay plays a key role in the maximal intensification performances, a parametric study on operating temperature would be interesting. It is known that a lower temperature generally increases solubility but also viscosity and reduces the diffusivity coefficient. The intensification strongly depends on the solvent temperature. Strategic parameters can be achieved though the study of gain and loss with temperature. Lastly, for a given gas mixture, the determination of specific solvent properties could be obtained with a process-design methodology.

The influence of solvent volatility, which has not been taken into account in this study, should also be considered. Methanol and water indeed show vapour pressure levels which induce solvent losses during the absorption process. Symmetrically, wet feed mixtures can also lead to water absorption effects when hydrophilic solvents, such as ionic liquids, are used. In that case multicomponent fluxes from and to the liquid phase should be considered. Interestingly, dense membranes (thin film composite or selfstanding) could offer attractive possibilities in order to limit the solvent losses. For the Rectisol (methanol) case, a dense polymer showing a large permeability towards CO₂ but a low permeability towards methanol would surely be of interest.

It is expected that this exploratory parametric study will stimulate further researches on intensified processes with physical solvents.

6. Funding

This research did not receive any specific grant from funding agencies in the public, commercial, or not-for-profit sectors.

7. References

- [1] P.H.M. Feron, A.E. Jansen, CO₂ separation with polyolefin membrane contactors and dedicated absorption liquids: performances and prospects, *Separation and Purification Technology*. 27 (2002) 231–242. [https://doi.org/10.1016/S1383-5866\(01\)00207-6](https://doi.org/10.1016/S1383-5866(01)00207-6).
- [2] A. Gabelman, S.-T. Hwang, Hollow fiber membrane contactors, *Journal of Membrane Science*. 159 (1999) 61–106. [https://doi.org/10.1016/S0376-7388\(99\)00040-X](https://doi.org/10.1016/S0376-7388(99)00040-X).
- [3] R. Bounaceur, C. Castel, S. Rode, D. Roizard, E. Favre, Membrane contactors for intensified post combustion carbon dioxide capture by gas–liquid absorption in MEA: A parametric study, *Chemical Engineering Research and Design*. 90 (2012) 2325–2337. <https://doi.org/10.1016/j.cherd.2012.05.004>.
- [4] S. Zhao, P.H.M. Feron, L. Deng, E. Favre, E. Chabanon, S. Yan, J. Hou, V. Chen, H. Qi, Status and progress of membrane contactors in post-combustion carbon capture: A state-of-the-art review of new developments, *Journal of Membrane Science*. 511 (2016) 180–206. <https://doi.org/10.1016/j.memsci.2016.03.051>.
- [5] E. Favre, H.F. Svendsen, Membrane contactors for intensified post-combustion carbon dioxide capture by gas–liquid absorption processes, *Journal of Membrane Science*. 407–408 (2012) 1–7. <https://doi.org/10.1016/j.memsci.2012.03.019>.
- [6] M.R.M. Abu-Zahra, L.H.J. Schneiders, J.P.M. Niederer, P.H.M. Feron, G.F. Versteeg, CO₂ capture from power plants: Part I. A parametric study of the technical performance based on monoethanolamine, *International Journal of Greenhouse Gas Control*. 1 (2007) 37–46. [https://doi.org/10.1016/S1750-5836\(06\)00007-7](https://doi.org/10.1016/S1750-5836(06)00007-7).
- [7] E. Chabanon, R. Bounaceur, C. Castel, S. Rode, D. Roizard, E. Favre, Pushing the limits of intensified CO₂ post-combustion capture by gas–liquid absorption through a membrane contactor, *Chemical Engineering and Processing: Process Intensification*. 91 (2015) 7–22. <https://doi.org/10.1016/j.cep.2015.03.002>.
- [8] E. Chabanon, B. Belaissaoui, E. Favre, Gas–liquid separation processes based on physical solvents: opportunities for membranes, *Journal of Membrane Science*. 459 (2014) 52–61. <https://doi.org/10.1016/j.memsci.2014.02.010>.
- [9] E. Chabanon, E. Favre, Membrane contactors for intensified gas-liquid absorption processes, in: *Comprehensive Membrane Science and Technology*, Elsevier, E. Drioli & L. Giorno, 2017: pp. 127–153.
- [10] S. Mokhatab, W.A. Poe, Chapter 7 - Natural Gas Sweetening, in: S. Mokhatab, W.A. Poe (Eds.), *Handbook of Natural Gas Transmission and Processing (Second Edition)*, Gulf Professional Publishing, Boston, 2012: pp. 253–290. <https://doi.org/10.1016/B978-0-12-386914-2.00007-8>.
- [11] V.Y. Dindore, D.W.F. Brilman, F.H. Geuzebroek, G.F. Versteeg, Membrane–solvent selection for CO₂ removal using membrane gas–liquid contactors, *Separation and Purification Technology*. 40 (2004) 133–145. <https://doi.org/10.1016/j.seppur.2004.01.014>.
- [12] V.Y. Dindore, D.W.F. Brilman, P.H.M. Feron, G.F. Versteeg, CO₂ absorption at elevated pressures using a hollow fiber membrane contactor, *Journal of Membrane Science*. 235 (2004) 99–109. <https://doi.org/10.1016/j.memsci.2003.12.029>.
- [13] J. Albo, P. Luis, A. Irbaien, Carbon Dioxide Capture from Flue Gases Using a Cross-Flow Membrane Contactor and the Ionic Liquid 1-Ethyl-3-methylimidazolium Ethylsulfate, *Ind. Eng. Chem. Res.* 49 (2010) 11045–11051. <https://doi.org/10.1021/ie1014266>.
- [14] P. Luis, Use of monoethanolamine (MEA) for CO₂ capture in a global scenario: Consequences and alternatives, *Desalination*. 380 (2016) 93–99. <https://doi.org/10.1016/j.desal.2015.08.004>.
- [15] I.P. Prevention, Control Reference Document on Best Available Techniques for the Manufacture of Large Volume Inorganic Chemicals-Ammonia, Acids and Fertilisers Dated on August. (2007).
- [16] B. Burr, L. Lyddon, B. Research, A COMPARISON OF PHYSICAL SOLVENTS FOR ACID GAS REMOVAL, 87th Annual Gas Processors Association Convention. (2008).
- [17] K. Li, W.K. Teo, An Ultrathin Skinned Hollow Fibre Module for Gas Absorption at Elevated Pressures, *Chemical Engineering Research and Design*. 74 (1996) 856–862. <https://doi.org/10.1205/026387696523157>.
- [18] A. Trusov, S. Legkov, L.J.P. van den Broeke, E. Goetheer, V. Khotimsky, A. Volkov, Gas/liquid membrane contactors based on disubstituted polyacetylene for CO₂ absorption liquid regeneration

- at high pressure and temperature, *Journal of Membrane Science*. 383 (2011) 241–249. <https://doi.org/10.1016/j.memsci.2011.08.058>.
- [19] O. Falk-Pedersen, M.S. Grønvold, P. Nøkleby, F. Bjerve, H.F. Svendsen, CO₂ Capture with Membrane Contactors, *International Journal of Green Energy*. 2 (2005) 157–165. <https://doi.org/10.1081/GE-200058965>.
- [20] R. Klaassen, P. Feron, A. Jansen, Membrane contactor applications, *Desalination*. 224 (2008) 81–87. <https://doi.org/10.1016/j.desal.2007.02.083>.
- [21] S. Li, D.J. Rocha, S. James Zhou, H.S. Meyer, B. Bikson, Y. Ding, Post-combustion CO₂ capture using super-hydrophobic, polyether ether ketone, hollow fiber membrane contactors, *Journal of Membrane Science*. 430 (2013) 79–86. <https://doi.org/10.1016/j.memsci.2012.12.001>.
- [22] * Josef Barthel, and Roland Neueder, H. Roch, Density, Relative Permittivity, and Viscosity of Propylene Carbonate + Dimethoxyethane Mixtures from 25 °C to 125 °C, (2000). <https://doi.org/10.1021/je000098x>.
- [23] M. Anouti, Y.R. Dougassa, C. Tessier, L. El Ouatani, J. Jacquemin, Low pressure carbon dioxide solubility in pure electrolyte solvents for lithium-ion batteries as a function of temperature. Measurement and prediction, *The Journal of Chemical Thermodynamics*. 50 (2012) 71–79. <https://doi.org/10.1016/j.jct.2012.01.027>.
- [24] F. Murrieta-Guevara, A. Romero-Martinez, A. Trejo, Solubilities of carbon dioxide and hydrogen sulfide in propylene carbonate, N-methylpyrrolidone and sulfolane, *Fluid Phase Equilibria*. 44 (1988) 105–115. [https://doi.org/10.1016/0378-3812\(88\)80106-7](https://doi.org/10.1016/0378-3812(88)80106-7).
- [25] M. DÍAZ, A. VEGA, J. COCA, Correlation for the Estimation of Gas-Liquid Diffusivity, *Chemical Engineering Communications*. 52 (1987) 271–281. <https://doi.org/10.1080/00986448708911872>.
- [26] C.R. Wilke, P. Chang, Correlation of diffusion coefficients in dilute solutions, *AIChE Journal*. 1 (1955) 264–270. <https://doi.org/https://doi.org/10.1002/aic.690010222>.
- [27] R.R. Wanderley, H.K. Knuutila, Mapping Diluents for Water-Lean Solvents: A Parametric Study, *Ind. Eng. Chem. Res*. 59 (2020) 11656–11680. <https://doi.org/10.1021/acs.iecr.0c00940>.
- [28] W. Schotte, Prediction of the molar volume at the normal boiling point, *The Chemical Engineering Journal*. 48 (1992) 167–172. [https://doi.org/10.1016/0300-9467\(92\)80032-6](https://doi.org/10.1016/0300-9467(92)80032-6).
- [29] B.E. Poling, J.M. Prausnitz, J.P. O’Connell, *Properties of Gases and Liquids*, Fifth Edition, McGraw-Hill Education: New York, Chicago, San Francisco, Athens, London, Madrid, Mexico City, Milan, New Delhi, Singapore, Sydney, Toronto, 2001. /content/book/9780070116825 (accessed December 9, 2019).
- [30] A.C. Ritchie, K. Bowry, A.C. Fisher, J.D.S. Gaylor, A novel automated method for the determination of membrane permeability in gas-liquid transfer applications, *Journal of Membrane Science*. 121 (1996) 169–174. [https://doi.org/10.1016/S0376-7388\(96\)00174-3](https://doi.org/10.1016/S0376-7388(96)00174-3).
- [31] S. Heile, S. Rosenberger, A. Parker, B. Jefferson, E.J. McAdam, Establishing the suitability of symmetric ultrathin wall polydimethylsiloxane hollow-fibre membrane contactors for enhanced CO₂ separation during biogas upgrading, *Journal of Membrane Science*. 452 (2014) 37–45. <https://doi.org/10.1016/j.memsci.2013.10.007>.
- [32] Y. Li, L. ’ao Wang, P. Jin, X. Song, X. Zhan, Removal of carbon dioxide from pressurized landfill gas by physical absorbents using a hollow fiber membrane contactor, *Chemical Engineering and Processing: Process Intensification*. 121 (2017) 149–161. <https://doi.org/10.1016/j.cep.2017.09.004>.
- [33] S.-J. Kim, A. Park, S.-E. Nam, Y.-I. Park, P.S. Lee, Practical designs of membrane contactors and their performances in CO₂/CH₄ separation, *Chemical Engineering Science*. 155 (2016) 239–247. <https://doi.org/10.1016/j.ces.2016.08.018>.
- [34] E. Chabanon, D. Roizard, E. Favre, Modeling strategies of membrane contactors for post-combustion carbon capture: A critical comparative study, *Chemical Engineering Science*. 87 (2013) 393–407. <https://doi.org/10.1016/j.ces.2012.09.011>.
- [35] B. Belaissaoui, J. Claveria-Baro, A. Lorenzo-Hernando, D. Albarracin Zaidiza, E. Chabanon, C. Castel, S. Rode, D. Roizard, E. Favre, Potentialities of a dense skin hollow fiber membrane contactor for biogas purification by pressurized water absorption, *Journal of Membrane Science*. 513 (2016) 236–249. <https://doi.org/10.1016/j.memsci.2016.04.037>.

- [36] L.P.B.M. Janssen, M.M.C.G. Warmoeskerken, *Transport Phenomena Data Companion*, Edward Arnold, 1987.
- [37] S. Kartohardjono, V. Chen, Mass Transfer and Fluid Hydrodynamics in Sealed End Hydrophobic Hollow Fiber Membrane Gas-liquid Contactors, *Journal of Applied Membrane Science & Technology*. 2 (2017). <https://doi.org/10.11113/amst.v2i1.1>.
- [38] J.S. Eckert, A new look at distillation tower packings comparative performance, *Chem. Eng. Prog.*, 1963.
- [39] R. Billet, M. Schultes, Prediction of Mass Transfer Columns with Dumped and Arranged Packings: Updated Summary of the Calculation Method of Billet and Schultes, *Chemical Engineering Research and Design*. 77 (1999) 498–504. <https://doi.org/10.1205/026387699526520>.